Integrated Optimal Siting and Sizing for VSC-HVDC-link-based Offshore Wind Farms and Shunt Capacitors

Yong Li, Xuebo Qiao, Chun Chen, Yi Tan, Wenchao Tian, Qiuping Xia, Yijia Cao, and Kwang Y. Lee

***Abstract*—It is economic and secure to determine the optimal siting and sizing of the offshore wind farms (OWFs) integrated into the AC system through voltage-source converter high-voltage direct current (VSC-HVDC) links. In this paper, an integrated planning model for the VSC-HVDC-link-based OWFs and the capacitors is proposed, where a decomposition technique is presented to solve the proposed mixed-integer nonlinear programming (MINLP) problem and obtain the optimal solution. This model can optimize the siting and sizing of the OWFs to improve the voltage profile and reduce the adverse influence of the reactive power of the OWFs. With the proposed planning model, the total investment costs, operation costs and maintenance costs of the OWFs, VSC-HVDC links, and the capacitors can be minimized. Simulations on the modified IEEE 118-bus system show that the proposed integrated planning model can provide more economic scheme than the independent planning scheme, in which the capacitors are planned after the OWFs. Besides, a series of sensitivity analysis on certain equipment costs are studied to obtain the regular pattern for sizing VSC stations.**

***Index Terms*—Capacitor, installed capacity, point of common coupling (PCC), offshore wind farm (OWF), voltage-source converter high-voltage direct current (VSC-HVDC) link.**

I. Introduction

ENVIRONMENT-FRIENDLY society has been emphasized increasingly all over the world, calling for renewable energy such as wind and solar energy generations [1], [2]. Moreover, the application of renewable energy is one of the best ways to protect the environment by reducing the carbon emissions [1]. Compared with the onshore wind farms, offshore wind farms (OWFs) have remarkable advantages such as higher wind speed and less noise [3]. Therefore, many OWFs have been constructed in recent years, for example, the German projects of HelWin2 (800 MW) and Dolwin2 (900 MW) in 2015 [4]. In the near future, it is promising that more OWFs will be connected to the onshore AC system so as to alleviate the energy shortage [5].

The optimal siting and sizing of OWFs can provide the economic and security operation of power systems, i.e., decreasing the total investment and operation costs of the OWFs and voltage-source converter high-voltage direct current (VSC-HVDC) links. Many approaches have been suggested for the siting and sizing of wind farms. In [6], a power loss reduction method is proposed to identify the optimal point of common coupling (PCC) of wind farm in the AC system. However, the sizing of wind farm is not optimized. In [7], the optimal sizing of wind farm under the given sites and the total penetration level is scheduled for maximizing the transient voltage stability level and operation benefit. Reference [8] optimizes the siting of OWFs for maximizing the energy production and minimizing the total investment with consideration of wake effect. In [9], a detailed technical and economic analysis is presented for different sizes of OWFs which are connected to the onshore grid through HVDC links. However, how to identify the optimal sizing of the OWFs is not discussed in [8] and [9].

VSC-HVDC transmission system has been widely applied in integrating OWFs into the onshore AC system due to its advantages such as no requirement of reactive power compensation (RPC) on the AC side of converters [10], independent and flexible control of active and reactive powers [11], and black start capability [12]. VSC-HVDC links of different capacities connected to different PCCs could result in different power losses and voltage profiles. In order to maximize the profit under given security constraints in transmission expansion planning, it is indispensable to identify the best siting of PCC to connect the VSC-HVDC link and determine the suitable sizing of OWFs to be connected to the AC system.

Manuscript received: October 21, 2018; accepted: January 29, 2020. Date of CrossCheck: January 29, 2020. Date of online publication: July 30, 2020.

This work was supported in part by the National Key Research and Development Program of China (No. 2016YFB0900100), in part by the National Natural Science Foundation of China (No. 51707059), in part by the 111 Project of China (No. B17016), and in part by the Excellent Innovation Youth Program of Changsha of China (No. KQ1802029).

Y. Li, X. Qiao, Y. Tan, and Y. Cao are with the College of Electrical and Information Engineering, Hunan University, Changsha 410082, China (e-mail: yongli@hnu.edu.cn; xbq1992@hnu.edu.cn; yitan@hnu.edu.cn; yjcao@hnu.edu.cn).

C. Chen (corresponding author) is with the School of Electrical and Information Engineering, Changsha University of Science and Technology, Changsha 410082, China (e-mail: chch3266@126.com).

W. Tian and Q. Xia are with the Zhangjiakou Power Supply Company, State Grid Jibei Electric Power Company Limited, Zhangjiakou 075000, China (e-mail: 2453753891@qq.com; 295581393@qq.com).

K. Y. Lee is with the Department of Electrical and Computer Engineering, Baylor University, Waco, Texas 76798-7356, USA (e-mail: kwang_y_lee@baylor.edu).

DOI: 10.35833/MPCE.2018.000538

With the direct integration of wind turbines, a poor voltage profile could be caused due to the reactive power absorption from AC system by the wind turbines, which can be considered as the source of voltage fluctuations [13]. When VSC-HVDC is used in integrating OWFs into onshore AC system, VSC station would compensate the reactive power required by the wind farm and maintain the voltage stability. However, the AC system still needs to provide RPC for improving the voltage in order to absorb offshore wind energy as much as possible when the loads increase annually. It means that the RPC device such as shunt capacitors can indirectly compensate the reactive power consumed by OWFs at the system level. To improve the voltage profile, appropriate sizes of capacitors are needed at appropriate sites in the AC system in transmission planning. Many researches have focused the optimal placement of capacitors in power systems [14]-[16] without considering the integrated planning of the shunt capacitors and the VSC-HVDC-link-based OWFs in transmission system.

Therefore, an integrated planning model for the VSC-HVDC-link-based OWFs and the shunt capacitors is proposed. The contributions of the proposed planning model are listed as follows: ① the best siting and sizing of the VSC-HVDC-link-based OWFs and the capacitors can be obtained, and the adverse influences of the reactive power of OWFs can be improved; ② a decomposition technique is presented to solve the proposed mixed-integer nonlinear programming (MINLP) problem and obtain the optimal solution. Moreover, the optimal total investment cost, operation cost and maintenance cost of OWFs can be obtained in the integrated planning model.

The rest of the paper is organized as follows. In Section II, the mathematical model from the aspects of objective function and the models of the wind generators, the VSC-HVDC, the AC power system, and the capacitors are introduced. The methodology to solve the proposed integrated planning model is described in Section III. Case studies are used to validate the proposed model in Section IV. A brief conclusion is given in Section V.

II. Optimal Siting and Sizing Model of VSC-HVDC-link-based OWF

We aim to optimize the connection point and the sizing of the VSC-HVDC-link-based OWFs together with the shunt capacitors to achieve the economic planning. Taking the AC-DC system in Fig. 1 as an example, the sizing of OWFs and HVDC, the siting of PCC 1 and PCC 2 (the connection points of OWF 1 and OWF 2, respectively), and the sizing and siting of the shunt capacitors will be optimized together.

A. Objective Function

Considering the power consumption, installation cost, operation cost, and maintenance cost in a planning period, the objective function of the proposed integrated planning model can be formulated as:

$$Obj = C_{sale} - C_W - C_{vsc} - C_{cab} - C_{cap} - C_p \tag{1}$$

where Obj is the total economic benefits with the unit; C_{sale} is the income of total electricity sale; and C_w, C_{vsc}, C_{cab}, C_{cap}, and C_p are the total costs of OWFs, VSC stations, HVDC cables, capacitors, and generation costs of all power plants in AC system, respectively. Note that C_w, C_{vsc}, C_{cab}, and C_{cap} include the investment cost, installation cost, operation cost, and maintenance cost. Present value of total earning of grid operator is considered for calculating the total benefit for a planning period of T_y years.

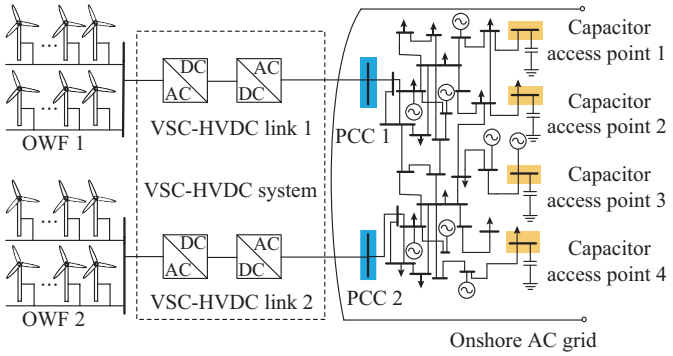

Fig. 1. Example system with VSC-HVDC-link-based OWFs and capacitors.

1) Total Electricity Sale

$$C_{sale} = \sum_{t=1}^{T_y}\sum_{i=1}^{n}\frac{1}{(1+\xi)^t}P_{i,load}(t)C_eT_h \tag{2}$$

where ξ is the discount rate; t and i are the indices of year and AC buses, respectively; n is the number of AC buses; C_e is the electricity price; T_h is equal to 8760 hours; and $P_{i,load}(t)$ is the average hourly active power load at AC bus i.

2) Total Cost of Wind Farms

$$C_W = \sum_{\substack{l\in\Omega_{OWF}\\ k\in\Omega_{PCC}}} u_{lk}C_W^{in}J_{lk,W} + \sum_{t=1}^{T_y}\sum_{\substack{l\in\Omega_{OWF}\\ k\in\Omega_{PCC}}}\frac{1}{(1+\xi)^t}u_{lk}C_W^{o}E_{lk}(t) \tag{3}$$

where Ω_{OWF} and Ω_{PCC} are the sets of OWF candidates and total PCC candidates of all OWFs, respectively; u_{lk} is a binary variable, and $u_{lk}=1$ and $u_{lk}=0$ represent the OWF l is connected and disconnected to the PCC k, respectively; C_W^{in} is the sum of the per-unit capacity investment and installation costs of OWF; C_W^0 is the sum of per-unit capacity operation and maintenance costs of OWF; $J_{lk,W}$ is the installed capacity of OWF l connected to the possible PCC k; and $E_{lk}(t)$ is the total energy generation of the OWF l connected to the PCC k in year t.

In fact, the output of OWF is not fixed due to weather condition. Considering the average hourly output, the wind energy generation of year t, $E_{lk}(t)$ can be calculated as:

$$E_{lk}(t) = T_h P_{lk,W}^{cre} \tag{4}$$

where $P_{lk,W}^{cre}$ is the average hourly output of the OWF l connected to the PCC k. It can be calculated by:

$$P_{lk,W}^{cre} = \eta_l J_{lk,W} \tag{5}$$

where η_l is the capacity factor (CF) [17], and it is an average for one year.

3) Total Cost of VSC Stations

$$C_{vsc}=\sum_{\substack{l\in\Omega_{OWF}\\k\in\Omega_{PCC}}}u_{lk}(C_{vsc,in}^{off}+C_{vsc,in}^{on})J_{lk,vsc}+\sum_{t=1}^{T_y}\sum_{\substack{l\in\Omega_{OWF}\\k\in\Omega_{PCC}}}\frac{1}{(1+\xi)^t}u_{lk}(M_{lk,vsc}^{off}+M_{lk,vsc}^{on}) \tag{6}$$

where $C_{vsc,in}^{off}$ and $C_{vsc,in}^{on}$ are the sum of per-unit capacity investment and installation costs of offshore and onshore VSC station, respectively; $J_{lk,vsc}$ is the MVA rating of the VSC station connecting the OWF l to the PCC k; and $M_{lk,vsc}^{off}$ and $M_{lk,vsc}^{on}$ are the annual total operation and maintenance costs of offshore and onshore VSC stations, respectively. In this paper, it is assumed that the installed capacity of VSC station is directly proportional to the corresponding OWF of the installed capacity to allow reactive power transfers if needed.

4) Total Cost of HVDC Cables

$$C_{cab}=\sum_{\substack{l\in\Omega_{OWF}\\k\in\Omega_{PCC}}}u_{lk}C_{cab}^{in}d_{lk}+\sum_{t=1}^{T_y}\sum_{\substack{l\in\Omega_{OWF}\\k\in\Omega_{PCC}}}\frac{1}{(1+\xi)^t}u_{lk}M_{lk,cab}^{o} \tag{7}$$

where C_{cab}^{in} is the per-unit length investment and installation cost of HVDC cable; d_{lk} is the cable distance of HVDC link connecting the OWF l to the PCC k; and $M_{lk,cab}^{o}$ is the annual maintenance cost of HVDC cable. The first item at the right-hand side of (7) means the investment and installation costs of the HVDC cable and the second part represents the maintenance and operation costs of the HVDC cable.

5) Total Cost of Capacitors

$$C_{cap}=\sum_{i=1}^{n}u_iC_{cap}^{in}Q_{i,cap}+\sum_{t=1}^{T_y}\sum_{i=1}^{n}\frac{1}{(1+\xi)^t}u_iM_{i,cap}^{o} \tag{8}$$

where C_{cap}^{in} is the per-unit capacity investment and installation cost of capacitors; $Q_{i,cap}$ is the installed capacity of capacitors at AC bus i; u_i is the binary variable, and u_i=1(0) means that capacitors are (not) sited in bus i; and $M_{i,cap}^{o}$ is the annual total operation and maintenance cost of capacitors installed at bus i. The first item at the right-hand side of (8) describes the investment and installation cost of the capacitors, and the second one represents the maintenance and operation cost of the capacitors.

6) Total Generation Cost of Power Plants in AC System

$$C_p=\sum_{t=1}^{T_y}\sum_{i=1}^{n}\frac{1}{(1+\xi)^t}(a_iP_{i,g}^2(t)+b_iP_{i,g}(t)+c_i)T_h \tag{9}$$

B. OWF Constraints

The installed capacity of OWFs should satisfy the following constraints:

$$J_{l,w}^{\min}\le J_{l,w}\le J_{l,w}^{\max} \tag{10}$$

where $J_{l,w}^{\min}$ and $J_{l,w}^{\max}$ are the minimum and maximum installed capacities of OWF l, respectively. We assume $J_{l,w}^{\min}=0$.

The reactive output $Q_{l,w}(t)$ of OWFs should satisfy:

$$Q_{l,w}^{\min}\le Q_{l,w}(t)\le Q_{l,w}^{\max} \tag{11}$$

The configurations of the two terminal VSC-HVDC systems, which have been adopted in some applications, are investigated in this paper. Furthermore, it is assumed that the OWF l is connected to the PCC k only by one VSC-HVDC link. Therefore, the following equations should be satisfied:

$$\sum_{k\in\Omega_{PCC}}u_{lk}=1 \tag{12}$$

$$\sum_{\substack{l\in\Omega_{POWF}\\k\in\Omega_{PCC}}}u_{lk}=m \tag{13}$$

where m is the number of OWFs in the planning. In addition, k and m in (12) and (13) should be modified when the OWF connecting to the PCC k is linked by the VSC-MTDC system, and it is decided by the given VSC-MTDC topology.

C. VSC-HVDC Model

For a pulse width modulation (PWM) based VSC-HVDC system, it includes VSCs, phase reactors, AC filters and transformers which are used to connect the OWF to the AC system, as shown in Fig. 2 [18].

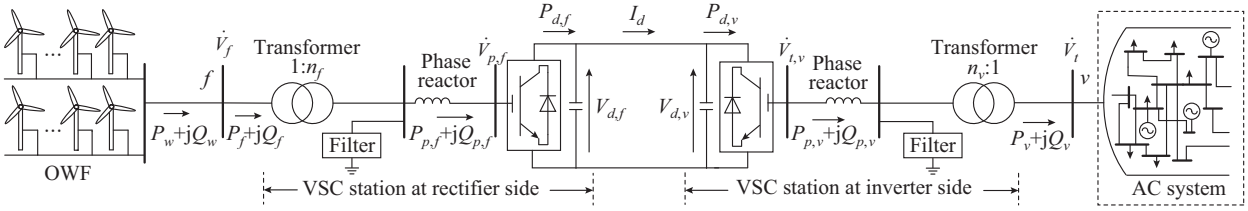

Fig. 2. Single phase diagram for PWM based VSC-HVDC link connecting OWF and onshore AC system [19].

The filters can be eliminated when multilevel modular converter (MMC) technology is used in VSC-HVDC [19]. In this paper, only MMC-based VSC-HVDC system will be investigated and thus the impedances of the phase reactor and the transformer can be combined as an equivalent Z_β to simplify the optimal power flow calculation.

In Fig. 2, it is regarded that active power output of OWFs P_w and reactive power output of OWFs Q_w are equal to the power flows P_f and Q_f, respectively; P_β and Q_β are the active and reactive power injected into the VSC station, respectively; and $P_{p,\beta}$ and $Q_{p,\beta}$ are the active and reactive power injected into the AC bus of VSC converter, where $\beta=f,v$, and f is the rectifier, and v is the inverter. The formulation of P_β, Q_β, $P_{p,\beta}$, and $Q_{p,\beta}$ are given in [20]. For the DC side, the voltages and currents can be calculated as [20]:

$$I_d(t)=\frac{U_{d,f}(t)-U_{d,v}(t)}{R_d} \tag{14}$$

$$U_{d,\beta}(t)=\frac{2\sqrt{2}\,U_{p,\beta}(t)}{M_\beta(t)} \tag{15}$$

$$P_{d,\beta}(t)=U_{d,\beta}(t)I_d(t) \tag{16}$$

where $I_d(t)$ and $U_{d,\beta}(t)$ are the direct current of HVDC cable and DC voltage at DC bus of VSC converter in year t, respectively; and $U_{p,\beta}(t)$ is voltage magnitude at AC bus of VSC converter in year t. Equation (15) depicts that the DC voltage of HVDC system can be adjusted by the amplitude modulation ratio $M_\beta(t)$.

In addition, the inequality constraints are required for $P_{p,\beta}(t)$, $Q_{p,\beta}(t)$, $U_\beta(t)$, $U_{p,\beta}(t)$, $\theta_\beta(t)$, $\theta_{p,\beta}(t)$, $U_{p,\beta}(t)$, and $I_d(t)$ to guarantee that they are within certain limits.

D. AC System Model

When assuming that the shunt capacitor banks would not be adjustable, the power flow equation at each AC bus i ($i \in \Omega$) can be expressed as:

$$P_{i,p}(t) - P_{i,load}(t) = U_i(t) \sum_{j=1}^{n} U_j(t)(G_{ij}\cos\theta_{ij}(t) + B_{ij}\sin\theta_{ij}(t)) \tag{17}$$

$$Q_{i,p}(t) + u_i Q_{i,cap} - Q_{i,load}(t) = U_i(t) \sum_{j=1}^{n} U_j(t)(G_{ij}\sin\theta_{ij}(t) - B_{ij}\cos\theta_{ij}(t)) \tag{18}$$

where $P_{i,load}(t)$ and $Q_{i,load}(t)$ are the average hourly active and reactive power loads at AC bus i in year t, respectively; $U_i(t)$ and $U_j(t)$ are the voltage magnitudes at AC buses i and j in year t, respectively; G_{ij} and B_{ij} are the conductance and susceptance elements of AC system admittance matrix, respectively; $\theta_{ij}(t)$ is the phase angle difference between bus i and bus j in year t; and $Q_{i,cap}$ is the reactive power supported by the shunt capacitor banks at AC bus i. Considering that the installed capacitors have discrete property, it can be expressed as:

$$Q_{i,cap} = g_i Q_{0,cap} \tag{19}$$

where $Q_{0,cap}$ is the unit capacity of the capacitor bank; and g_i is an integer variable, representing the number of unit capacitors of the capacitor bank. In (19), the shunt capacitor bank is formulated as a constant reactive power sources. At the inverter side of VSC in Fig. 2, the power flow $P_v^{inj}(t)$ and $Q_v^{inj}(t)$ injected into the bus v can be formulated as:

$$P_v^{inj}(t) = P_{v,g}(t) - u_{lv}P_v(t) - P_{v,load}(t) \tag{20}$$

$$Q_v^{inj}(t) = Q_{v,g}(t) + u_v Q_{v,cap} - u_{lv}Q_v(t) - Q_{v,load}(t) \tag{21}$$

Generation output limits, bus voltage and phase angle limits, branch power flow limits, as well as the lower and upper limits for the number of unit capacitors of the capacitor bank are listed as follows:

$$\begin{cases} P_{i,g}^{\min}(t) \le P_{i,g}(t) \le P_{i,g}^{\max}(t) \\ Q_{i,g}^{\min}(t) \le Q_{i,g}(t) \le Q_{i,g}^{\max}(t) \\ U_i^{\min}(t) \le U_i(t) \le U_i^{\max}(t) \\ \theta_i^{\min}(t) \le \theta_i(t) \le \theta_i^{\max}(t) \\ S_{ij}(t) \le S_{ij}^{\max}(t) \end{cases} \tag{22}$$

where $S_{ij}(t)$ is the average hourly power flow of AC transmission line ij in year t. In addition, the number of installed capacitor sites is limited by (23), where n_{cap} is the maximum number of installation sites in AC system.

$$0 \le \sum_{i=1}^{n} u_i \le n_{cap} \tag{23}$$

In this paper, all AC buses are the possible connection points for installing capacitors. The reactive power generation can be changed from the AC buses by connecting to capacitor banks. The type of AC buses may also be changed due to the capacitor connections. Thus, to simplify the calculation process, the status and control variables of AC buses are constrained by equality and inequality constraints. And this concept has been demonstrated without defined slack bus [21].

E. Power Relationship Between OWFs and AC System

As shown in Fig. 2, VSC-HVDC system is used in integrating OWFs into AC system. In order to receive wind energy as much as possible in AC system, the VSC station at the OWF side generally adopts the control mode of constant active power and constant AC voltage (P_f, U_f control), and the $U_{d,f}(t)$ would be also constant by (15). Neglecting the active power loss of converters, it is regarded that the active power injected to the VSC converter and PCC in the onshore AC system is equal to the DC power [20]. Thus, the power flow equations are:

$$P_{d,f}(t) = P_w(t) \tag{24}$$

$$P_{d,v}(t) = P_v(t) = P_{PCC}(t) \tag{25}$$

$$Q_{d,f}(t) = Q_w^{HVDC}(t) = \frac{U_f(t)}{X_{f,w}}\left[U_w(t)\cos(\theta_w(t) - \theta_f(t)) - U_f(t)\right] \tag{26}$$

$$Q_v(t) = \frac{U_{PCC}(t)}{X_{v,PCCk}}\left[U_{PCC}(t)\cos(\theta_{PCC}(t) - \theta_v(t)) - U_v(t)\right] \tag{27}$$

$$Q_{i,AC}(t) = \frac{U_{i,AC}(t)}{X_{PCC,i,AC}}\left[U_{i,AC}(t) - U_{PCC}(t)\cos(\theta_{i,AC}(t) - \theta_{PCC}(t))\right] \tag{28}$$

where $X_{f,w}$ is the reactance between HVDC and OWFs; $X_{PCC,i,AC}$ is the reactance between PCC and AC bus i connected to PCC; $Q_w^{HVDC}(t)$ is the reactive power of OWFs received to the rectifier terminal of HVDC; and $Q_{i,AC}(t)$ is the reactive power output of bus i in AC system delivered to the PCC. And the relation between $P_{PCC}(t)$ and $P_w(t)$ in (29) can be obtained by combining (14), (15), (16), (24) and (25), where $P_{PCC}(t)$ means the active power of PCC transferred to the onshore AC system.

$$P_{PCC}(t) = P_v(t) = P_w(t)\left(1 - \frac{P_w(t)}{U_{d,f}(t)^2}\right) \tag{29}$$

In addition, at least one VSC at the AC system side should adopt constant DC voltage control ($U_{d,v}$ control), which can be able to adjust the DC voltage. Then, the rest of VSC can be used for power regulation. Assuming that the remaining VSC adopts the control mode of constant AC voltage control (U_v control) and n_v is the transformer ratio at the VSC inverter side, $U_v(t)$ can be expressed by (30) with the combination of (14), (15), (16), (24) and (25).

$$U_v(t)=\frac{M_i}{2\sqrt{2}\,n_v}\left(U_{d,f}(t)-\frac{P_w(t)R_d}{U_{d,f}(t)}\right) \tag{30}$$

$$Q_{i,AC}(t)=\frac{U_{i,AC}(t)}{X_{PCC,i,AC}}\left[U_{i,AC}(t)-\frac{M_i}{2\sqrt{2}\,n_v}\left(U_{d,f}(t)-\frac{P_w(t)R_d}{U_{d,f}(t)}\right)\cdot \cos(\theta_{i,AC}(t)-\theta_{PCC}(t))\right] \tag{31}$$

Then, (31) can be obtained by combining (27) and (29) when assuming $U_{PCC}(t)=U_v(t)$, which shows that the reactive power output of AC system $Q_{AC}(t)$ is related to the active power output of OWFs $P_w(t)$. To absorb more electricity $P_v(t)$ from the inverter terminal of VSC-HVDC, $Q_{AC}(t)$ should be supplied by the AC system. And the shunt capacitors can be used as RPC device to compensate the reactive power in the AC system. Thus, we optimize the shunt capacitors together with the planning of VSC-HVDC-link-based OWFs.

In addition, there are similar power relationships between OWFs and onshore AC system in other control mode of VSC.

F. Decision Variables

In this paper, the decision variables include the installation sites and installed capacity of OWFs and the corresponding VSC stations as well as the sites and capacities of capacitor banks. In addition, the DC voltage and amplitude modulation of VSC-HVDC links and the outputs of thermal power plants during the planning period are also optimized.

III. Methodology

The proposed integrated planning model is an MINLP problem, which is not easy to be directly solved. Therefore, a decomposition technique is proposed.

Firstly, it is assumed that the sites of those OWFs satisfying the geological conditions are known. In practice, the set $\Omega_{PCC,l}$ is given in advance due to the actual conditions such as transmission length. Then, the optimal PCC of the OWF l will be selected from the given PCC set $\Omega_{PCC,l}$, where $\Omega_{PCC,l}$ ($l=1,2,...,m$) is the set of PCC candidates for the OWF l. It is also assumed that there is no overlapping among the sets of PCCs between each OWF. Therefore, the following equations should be stratified:

$$\sum_{l=1}^{m} N_l = N \tag{32}$$

$$\Omega_{PCC,1}\cup\Omega_{PCC,2}\cup\ldots\cup\Omega_{PCC,l}\cup\ldots\cup\Omega_{PCC,m}=\Omega_{PCC} \tag{33}$$

where N_l is the number of elements in the set $\Omega_{PCC,l}$. Since N_l is small in practice, a decomposition technique is proposed as shown in Fig. 3. The main idea of the proposed approach is to decompose the original non-convex model into several sub-MINLP problems with less integer variables. In each sub-problem, the binary variable u_{lk} is fixed and thus the number of integer variables is reduced. A series of sub-MINLP problems can be enumerated due to a limited number of PCCs connected to the VSC-HVDC links.

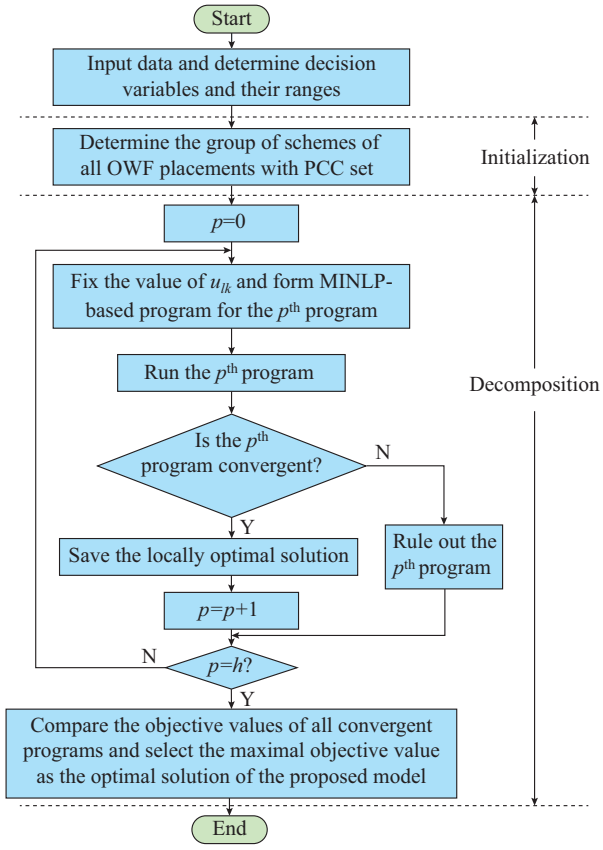

Fig. 3. Example system with VSC-HVDC based OWFs and capacitors.

IV. Case Studies

In this section, the proposed integrated planning model is validated on the modified IEEE 118-bus system, and general algebraic modeling system (GAMS) [22] is used to solve the proposed method. In this paper, two OWFs are considered. The candidate sets of the two OWFs are $\Omega_{PCC,1}$ and $\Omega_{PCC,2}$, which correspond to the upper and lower shadow boxes in Fig. 4, respectively. OWFs will be connected to one of the PCCs through their VSC-HVDC links, whose candidates are depicted with dotted line in Fig. 4. All the AC buses can be considered as the candidate for the installation of capacitors.

The unit cost of DC cable and the maintenance cost of VSC-HVDC are calculated based on [23]. The limits of I_d, U_β and M_β are cited from [24]. With reference to [7], to transfer the reactive power, this paper assumes that the installed capacity of VSC station is 1.2 times as large as the installed capacity of the corresponding OWF. The parameters of both OWFs are described in Appendix A Table AI.

It is supposed that the annual system load growth is 4.7% during the planning period. The parameters are set based on [25], including first-year load values of the AC system, phase angle limitations of AC buses as well as the cost coefficients and output limitations of power plants. For capacitors, $M^{o}_{i,cap}$ is set to be 5% of the total investment and installation costs in every year. In this paper, four sites are selected arbitrarily to install capacitor banks. Some basic parameters about system planning are listed in Appendix A Table AII, where C_e, C^{in}_W, C^{o}_W, and ξ are assumed based on [26]; $C^{off}_{vsc,in}$ and $C^{on}_{vsc,in}$ are assumed based on [27]; and C^{in}_{cap} is assumed based on [28].

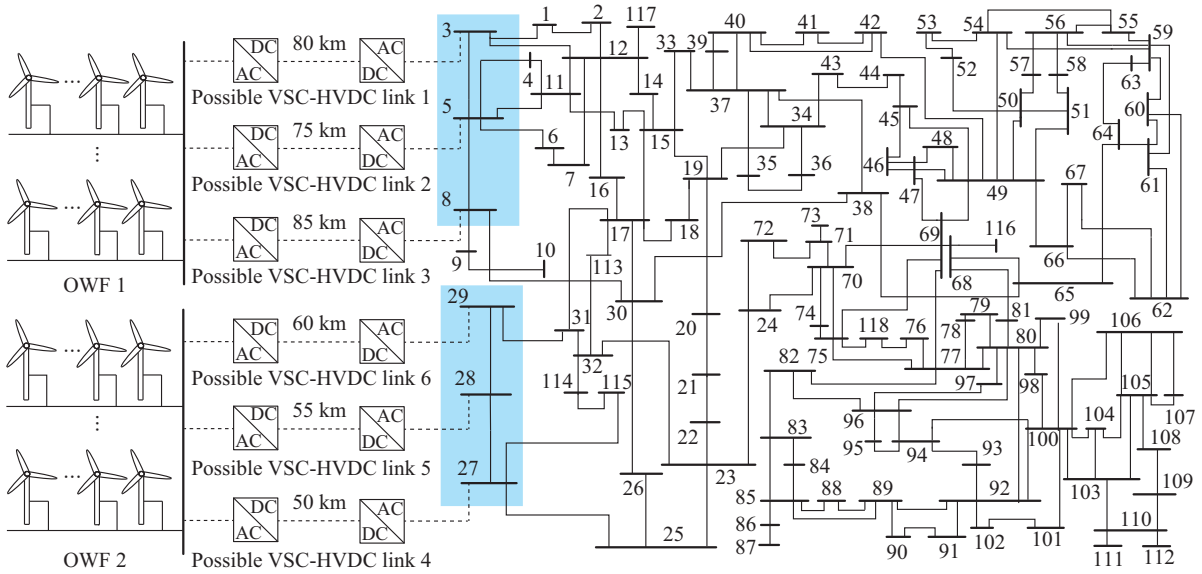

Fig. 4. Candidate VSC-HVDC link connecting OWF and IEEE 118-bus system.

A. Results Analysis of Three Cases

In this sub-section, Case A is the proposed method, and two cases are considered for comparison as follows.

1) Case B: single planning without capacitors, which is the only one connected to the AC system.

2) Case C: independent planning. The capacities of OWFs and VSC-HVDC links calculated from the case without capacitor planning are firstly fixed, and then the siting and sizing of capacitors are optimized in the system planning.

In this paper, both $\Omega_{PCC,1}$ and $\Omega_{PCC,2}$ contain three PCCs, then the original MINLP can be decomposed into 9 sub-MINLP problems with fixed value of u_{lk}. Nine schemes are depicted in Appendix A Table AIII.

The optimal solution cannot be obtained if the proposed integrated planning model is directly solved by MINLP due to the local infeasibility of the original program. In contrast, the optimal solution can be obtained through the proposed decomposition methodology. The computation time of the proposed methodology and the original method to solve the MINLP problem is listed in Table I. Thus, the proposed method can be more effective in solving the proposed integrated planning model compared with the original method.

TABLE I
COMPUTATION TIME TO SOLVE PROPOSED PLANNING MODEL BY DECOMPOSITION TECHNIQUE

Decomposition scheme	Time (s)	Decomposition scheme	Time (s)
1	2384	6*	
2	3397	7	2418
3*		8	1316
4	1749	9*	
5	2428		

Note: * represents that no solution is found.

Note that schemes 3, 6, and 9 are not considered in the following study because no feasible solutions are found by our program. However, optimal solutions for schemes 3, 6, and 9 can be found when enlarging the AC bus voltage limits, e.g., setting 0.88 and 1.12 p.u. as lower and upper limits, respectively. For other schemes, optimal solutions are also obtained. Using the proposed method, scheme 5 has the best total economic benefit, and bus 5 and bus 28 are the optimal PCCs to integrate OWF 1 and OWF 2 with VSC-HVDC link 2 and link 5, respectively. In contrast, scheme 8 has the best total benefit in the cases of independent planning and single planning without capacitors. Bus 8 and bus 28 are the optimal PCCs to integrate OWF 1 and OWF 2, respectively. VSC-HVDC link 3 and link 5 are the optimal VSC-HVDC links of OWF 1 and OWF 2 for the cases of independent planning and single planning without capacitors, respectively. Therefore, the optimal PCCs can be affected by the capacitor planning by comparison of the results of three cases. The main reason is that the appropriate sites to install capacitors can redistribute power flow to assist wind energy integration into the AC system.

In optimal scheme achieved by the proposed approach, VSC-HVDC link 5 is used. Note that the cable distance of HVDC 5 is longer than that of the HVDC 4. Thus, the selection of the optimal VSC-HVDC link is not in accordance with the distance principle, and it is comprehensively influenced by the distance of HVDC cable and the constraints of AC system.

Figure 5 shows that the proposed method has higher total benefit compared with the other two planning methods. The total economic benefits of independent planning obtain higher objective than that of the case of single planning without capacitors. For example, in scheme 5, the profit can be increased by 13 M€ if the capacitors and VSC-HVDC links are integrated into the AC system, as compared with the case of single planning without capacitors, which shows the advantages of the integrated planning.

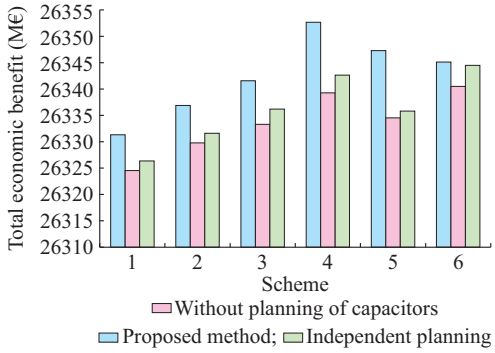

Fig. 5. Total economic benefit of different schemes of three cases.

In this paper, the installation capacity ratio (ICR) of OWF is defined to be equal to actual installation capacity divided by the maximum installation capacity of OWF. In Table II, it shows that ICR of OWF 1 is much higher than that of OWF 2, because CF of OWF 1 is higher than that of OWF 2 and its utilization ratio is higher. In Table III, the total size of capacitors of the proposed method is more than independent planning, which shows that the integrated planning demands of capacitors with a bigger size.

TABLE II
INSTALLED CAPACITY OF OWFS AND VSC STATIONS OF SCHEMES

Scheme	Case	OWF No.	OWF capacity (MW)	VSC station capacity (MVA)	ICR
1	A	1	911.841	1094.210	0.912
		2	380.270	456.324	0.475
	B	1	918.583	1102.300	0.919
		2	391.466	469.760	0.489
2	A	1	936.744	1124.092	0.937
		2	354.547	425.456	0.443
	B	1	944.464	1133.357	0.944
		2	362.241	434.689	0.453
4	A	1	1000.000	1200.000	1.000
		2	286.020	343.224	0.358
	B	1	1000.000	1200.000	1.000
		2	314.054	376.865	0.393
5	A	1	1000.000	1200.000	1.000
		2	275.292	330.351	0.344
	B	1	1000.000	1200.000	1.000
		2	304.176	365.011	0.380
7	A	1	1000.000	1200.000	1.000
		2	276.719	332.062	0.346
	B	1	1000.000	1200.000	1.000
		2	310.151	372.181	0.388
8	A	1	1000.000	1200.000	1.000
		2	302.336	362.804	0.378
	B	1	1000.000	1200.000	1.000
		2	307.198	368.638	0.384

The total energy output of power plants in AC system of the six schemes during 20 years is shown in Fig. 6. It shows that the total energy generation of power plants in the AC system of the proposed method is much higher than the other two cases, indicating that the appropriately installed capacitors can assist the utilization of the active power of generators in the AC system.

TABLE III
RESULTS OF OPTIMAL SITING AND SIZING OF CAPACITORS OF SCHEME 5

Case	Bus	Capacity (Mvar)
A	34	70
	35	20
	36	20
	118	90
B	3	20
	13	30
	34	50
	36	40

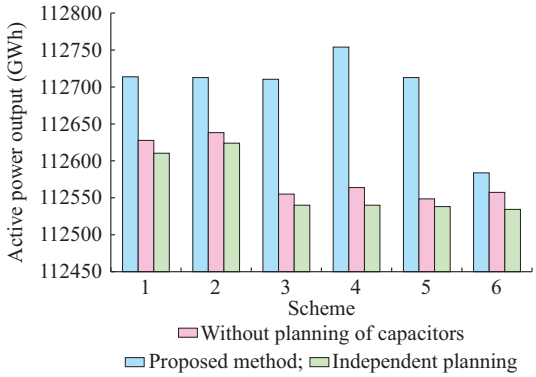

Fig. 6. Total energy output of generators in AC system during 20 years.

Pure reactive power generation is defined as the difference between reactive power generation (by power plants and shunt capacitor banks) and the reactive power absorption by VSC stations. Taking scheme 5 as an example, pure reactive power generation of the cases with the integration of capacitors will be higher than that of single planning without capacitors affected by the accession of large capacity capacitor banks into the AC system, as shown in Fig. 7. Pure reactive power generation of the proposed method is lower than that of independent planning. It proves an advantage in reducing the pure reactive power generation using the proposed method compared with independent planning.

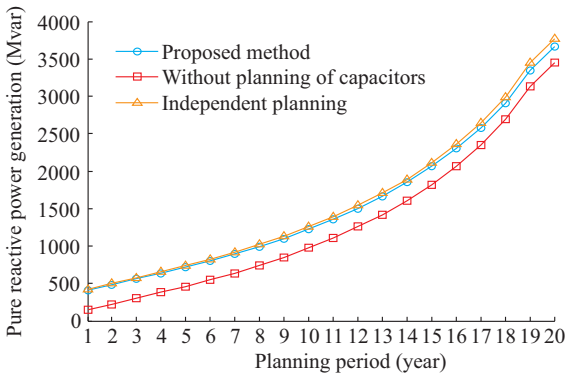

Fig. 7. Pure reactive power generation of scheme 5 in different planning periods.

Different load scenarios are used to investigate the optimal access point for connecting VSC-HVDC link in system planning with the annual load growth rate varying from 0.01 to 0.08 and an interval of 0.01. The total maximum power generations of power plants in the AC system are reset to adapt different annual load growth rate, which are modified based on the original generation share of each power plant in the AC system in [23].

Note that total benefits for schemes 3, 6, and 9 are not listed in Table IV. From Table IV, it is easily found that total benefits rise as the annual load growth rate increases. When annual load growth rate is lower than 0.01, the total benefits between the cases without capacitor planning and the proposed method are equal for each planning scheme. It is the reason that active and reactive power load demands are very low. Thus, the load demand can be easily compensated by power plants in AC system without adding operation cost in the AC system, which means that no shunt capacitor bank is required. When annual load growth rate is relatively higher, namely more than 0.02, it can be found that total benefits increase if shunt capacitors are planned together. And the benefit gap between the case of single planning without capacitors and the proposed planning method is apparent when the annual load growth rate is large enough, for example 0.07 and 0.08. It shows that the economic benefit of the proposed method is more remarkable when the annual load growth rate is much higher.

TABLE IV
TOTAL BENEFIT AND OPTIMAL SCHEMES FOR THREE CASES WITH DIFFERENT ANNUAL GROWTH RATE

Annual load growth rate	Maximum generation of power plants (MW)	Case	Total benefit (M€)					
			Scheme 1	Scheme 2	Scheme 4	Scheme 5	Scheme 7	Scheme 8
0.01	4730	A	20584.72	20586.61	20619.05	20623.25	20623.11	20627.38
		B	20584.72	20586.61	20619.05	20623.25	20623.11	20627.38
		C	20584.72	20586.61	20619.05	20623.25	20623.11	20627.38
0.02	5800	A	22094.15	22094.35	22120.80	22126.30	22125.89	22129.17
		B	22092.16	22094.29	22120.48	22124.52	22124.45	22128.59
		C	22092.54	22094.31	22120.68	22124.78	22124.68	22128.68
0.03	7100	A	23607.92	23603.85	23621.09	23626.24	23627.32	23629.87
		B	23599.14	23601.98	23620.44	23624.80	23623.84	23628.27
		C	23601.24	23602.34	23620.56	23625.19	23624.87	23628.68
0.04	8700	A	25208.61	25213.12	25222.12	25235.30	25224.60	25225.75
		B	25201.03	25205.94	25214.07	25219.87	25216.38	25222.20
		C	25203.56	25207.36	25215.85	25220.27	25217.08	25222.51
0.05	10600	A	26886.33	26901.03	26891.80	26898.61	26894.02	26898.43
		B	26876.68	26882.87	26881.81	26888.36	26882.85	26889.40
		C	26879.25	26893.56	26883.28	26892.59	26885.27	26898.00
0.06	12850	A	28657.29	28673.86	28663.78	28667.27	28656.14	Failed*
		B	28648.04	28655.70	28640.21	28648.05	28637.34	28645.25
		C	28652.74	28668.56	28650.18	28657.48	28642.59	Failed*
0.07	15600	A	30631.45	30627.89	30606.12	30593.81	30571.07	Failed*
		B	30594.26	30604.20	30558.00	30568.30	30544.78	30555.67
		C	30618.31	30619.57	30582.92	30575.64	30558.57	Failed*
0.08	18900	A	32734.10	32777.34	32629.19	32647.58	32638.26	Failed*
		B	32677.47	32694.26	32551.75	32572.35	Failed*	Failed*
		C	32706.51	32746.84	32597.47	32623.85	Failed*	Failed*

Note: * represents that the program is locally infeasible.

Moreover, from Table IV, optimal schemes are not the same due to different annual load growth rates. Affected by the integration of shunt capacitors, the optimal PCCs for connecting OWFs could be changed when the annual load growth rate is at 0.04, 0.05, and 0.07, respectively. Thus, accurate prediction for annual load growth rate is also important to plan both OWF and capacitors to obtain the maximum total benefit.

B. Sensitivity Analysis for System Planning

To evaluate which factor that could greatly influence the planning results, sensitivity analysis is employed based on the following parameters:

1) C_{cap}^{in} varies from 60% to 100% of the value given in Appendix A Table AII.

2) $Q_{0,cap}$ varies from 2 Mvar to 10 Mvar.

3) C_{W}^{in} varies from 60% to 100% of the value given in Table AII.

4) C_{vsc}^{in} for both offshore and onshore VSC stations varies from 60% to 110% of the value given in Appendix A Table AII.

5) $C_{w,vsc}^{in}$ varies from 60% to 100% of the value given in Appendix A Table AII.

6) C_{cab}^{in} of HVDC cable varies from 60% to 100% of the value given in Appendix A Table AII.

In order to study the influence of the parameters on the to-

tal benefits and optimal sizing for VSC-based OWF, scheme 5 is employed as the base method. The results of the sensitivity analysis on the scheme to obtain the planning results using the proposed parameters are shown in Tables V and VI and Figs. 8 and 9.

TABLE V
SENSITIVITY ANALYSIS: UNIT CAPACITY OF CAPACITOR BANK

$Q_{0,cap}$ (Mvar)	Total benefit (M€)	OWF No.	Capacity of OWF (MW)	Capacity of VSC station (MVA)	Site of capacitors	Capacity of capacitors (Mvar)
2	26348.957	1	1000.00	1200.00	Bus 13	30
					Bus 15	46
		2	278.30	333.96	Bus 38	172
					Bus 51	22
4	26342.948	1	1000.00	1200.00	Bus 43	28
					Bus 45	20
		2	300.47	360.56	Bus 51	24
6	26346.359	1	1000.00	1200.00	Bus 37	114
					Bus 53	90
		2	275.41	330.49	Bus118	90
8	26354.958	1	1000.00	1200.00	Bus 13	64
					Bus 19	88
		2	265.79	318.94	Bus 35	72
					Bus 76	88
10	26352.657	1	1000.00	1200.00	Bus 34	70
					Bus 35	20
		2	275.29	330.35	Bus 36	20
					Bus 118	90

TABLE VI
SENSITIVITY ANALYSIS: PER-UNIT LENGTH INVESTMENT AND INSTALLATION COST OF HVDC CABLE

C_{cab}^{in} (%)	Total benefit (M€)	OWF No.	Capacity of OWF (MW)	Capacity of VSC station (MVA)	Site of capacitors	Capacity of Capacitors (Mvar)
60	26383.584	1	1000.000	1200.000	Bus 33	30
					Bus 34	60
		2	288.935	346.722	Bus 36	30
					Bus 39	10
70	26373.743	1	1000.000	1200.000	Bus 35	30
					Bus 36	60
		2	291.104	349.217	Bus 93	40
80	26365.361	1	1000.000	1200.000	Bus 20	40
					Bus 35	30
		2	288.296	345.956	Bus 36	50
					Bus 44	20
90	26358.412	1	1000.000	1200.000	Bus 13	30
					Bus 15	70
		2	277.986	333.583	Bus 34	100
					Bus 70	60
100	26352.657	1	1000.000	1200.000	Bus 34	70
					Bus 35	20
		2	275.290	330.350	Bus 36	20
					Bus 118	90

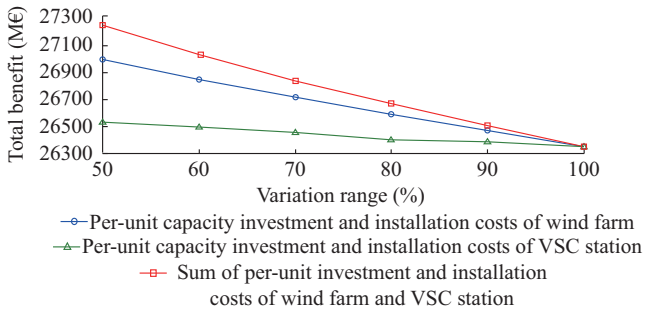

Fig. 8. Maximum total benefits of sensitivity analysis on C_{w}^{in}, C_{vsc}^{in}, and $C_{w,vsc}^{in}$.

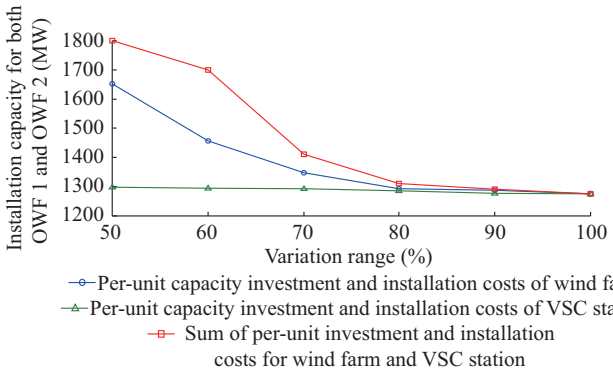

Fig. 9. Optimal installation capacity for OWF of sensitivity analysis on C_{w}^{in}, C_{vsc}^{in}, and $C_{w,vsc}^{in}$.

From the results of Tables V and VI and Figs. 8 and 9, the planning schemes are not changed as C_{cab}^{in} is varied. This is because the investment, installation and maintenance costs of capacitors are much less than the total benefit. Therefore, it can be inferred that (8) could be omitted in the proposed model. In contrast, both total benefits and installed capacity of VSC station can be influenced by the size of unit capacity of the capacitor bank. Also, optimal installation capacity and site of capacitor banks are different among the cases with different unit capacities of capacitor bank. This affects both active and reactive output of power plants in the AC system and installation capacities of OWF and VSC station. Therefore, unit capacity of capacitor bank can be also optimized to further maximize the total benefits.

With the maximum OWF installation capacity of nearly 16 MW, Table VI shows that the variation of the cost of HVDC cable has a limited impact on the sizing of OWF capacity. With the increase of C_{W}^{in}, C_{vsc}^{in}, and $C_{w,vsc}^{in}$, Fig. 8 shows that total benefits will be reduced and more significant influence can be caused by C_{W}^{in} as compared with C_{vsc}^{in} due to the higher investment and installation costs of OWF. In addition, the total installation capacities for both OWFs 1 and 2 will be reduced along with the increase of C_{W}^{in}, C_{vsc}^{in}, and $C_{w,vsc}^{in}$, as depicted in Fig. 9. Thus, the injection amount of offshore wind power could be increased by the lowering investment and installation costs. It should be noticed that installation capacities for both OWFs 1 and 2 reach the upper limits of 1000 MW and 800 MW, respectively, when C_{vsc}^{in} is set to be 50% of the one in Appendix A Table AII.

V. Conclusion

We propose a method for the optimal integrated siting and sizing of VSC-HVDC and capacitors for OWFs integrated power systems. The proposed decomposition approach is employed to determine the siting and sizing of capacitors and the VSC-HVDC-link-based OWFs. Simulations on the modified IEEE 118-bus system show that the selection of the optimal VSC-HVDC link is not just based on the proximity principle of OWF. It is comprehensively influenced by load levels, the distance of HVDC cable and constraints of AC system. More importantly, the proposed integrated planning method can provide more economic scheme as compared with the separate-planning approach in which the capacitors are planned after OWFs. Besides, the sensitivity analysis on the investment cost of different equipment shows that the installation capacity of OWF and VSC station can be raised significantly when the investment and installation cost of OWF and VSC is low enough. Furthermore, the application of the proposed method on the VSC-MTDC system and onshore wind farm will be the focus in our future research.

Appendix A

TABLE AI
Basic Parameters of Each OWF

OWF	$J_{l,w}^{\max}$ (MW)	$Q_{l,w}^{\max}$ (Mvar)	$Q_{l,w}^{\min}$ (Mvar)	CF
1	1000	300	–300	0.40
2	800	200	–200	0.36

TABLE AII
Basic Parameters for System Planning

Parameter	Value	Parameter	Value
C_e (€/MWh)	95	ξ	0.1
C_w^{in} (€/MW)	950000	$S_{ij}^{\max}$ (MVA)	800
C_w^o (€/MWh)	10	$Q_{0,cap}$ (Mvar)	10
$C_{vsc,in}^{off}$ (€/MVA)	141700	C_{cap}^{in} (€/Mvar)	20000
$C_{vsc,in}^{on}$ (€/MVA)	91700	$g_i^{\min}$	0
R_d (p.u./km)	5×10^{-5}	$g_i^{\max}$	120
Z_β (p.u.)	0.001+j0.01	$V_i^{\min}$ (p.u.)	0.9
T_y	20	$V_i^{\max}$ (p.u.)	1.1

TABLE AIII
Grouping on Possible Schemes by Decomposition Approach

Scheme	HVDC link (i,j)	Scheme	HVDC link (i,j)
1	1,4	6	2,6
2	1,5	7	3,4
3	1,6	8	3,5
4	2,4	9	3, 6
5	2,5		

References

[1] O. Noureldeen and I. Hamdan, "Design of robust intelligent protection technique for large-scale grid-connected wind farm," *Protection and Control of Modern Power Systems*, vol. 3, no. 1, pp. 169-182, Dec. 2018.

[2] S. Salman, X. Ai, and Z. Wu, "Design of a P&O algorithm based MPPT charge controller for a stand-alone 200 W PV system," *Protection and Control of Modern Power Systems*, vol. 3, no. 1, pp. 259-266, Dec. 2018.

[3] J. S. González, M. B. Payán, and J. R. Santos. "A new and efficient method for optimal design of large offshore wind power plants," *IEEE Transactions on Power Systems*, vol. 18, no. 3, pp. 3075-3084, Aug. 2013.

[4] J. Glasdam, J. Hjerrild, Ł. H. Kocewiak *et al*., "Review on multi-level voltage source converter based HVDC technologies for grid connection of large offshore wind farms," in *Proceedings of 2012 IEEE International Conference on Power System Technology (POWERCON)*, Auckland, New Zealand, Nov. 2012, pp. 1-6.

[5] S. K. Chaudhary, R. Teodorescu, and P. Rodriguez, "Wind farm grid integration using VSC based HVDC transmission – an overview," in *Proceedings of IEEE Energy 2030 Conference*, Atlanta, USA, Nov. 2008, pp. 1-7.

[6] I. M. Moreno, A. Median, and R. C. Magaña, "Methodology for optimal bus placement to integrate wind farm optimizing power flows," in *Proceedings of 2015 IEEE International Autumn Meeting on Power, Electronics and Computing (ROPEC)*, Ixtapa, Mexico, Nov. 2015, pp. 1-6.

[7] E. Mashayekhi and M. R. Aghamohammadi, "Transient voltage stability constrained optimal sizing of wind farm considering uncertainty of wind speed," in *Proceedings of 2014 22nd Iranian Conference on Electrical Engineering (ICEE)*, Tehran, Iran, May 2014, pp. 774-781.

[8] P. Hou, W. Hu, M. Soltani *et al*., "Optimized placement of wind turbines in large-scale offshore wind farm using particle swarm optimization algorithm," *IEEE Transactions on Sustainable Energy*, vol. 6, no. 4, pp. 1272-1282, Oct. 2015.

[9] P. Bresesti, W. L. Kling, R. L. Hendriks *et al*., "HVDC connection of offshore wind farms to the transmission system," *IEEE Transactions on Energy Conversion*, vol. 22, no. 1, pp. 37-43, Mar. 2007.

[10] P. Mitra, L. Zhang, and L. Harnefors, "Offshore wind integration to a weak grid by VSC-HVDC links using power-synchronization control: a case study," *IEEE Transactions on Power Delivery*, vol. 29, no. 1, pp. 453-461, Feb. 2014.

[11] H. Liu and Z. Chen, "Impacts of large-scale offshore wind farm integration on power systems through VSC-HVDC," in *Proceedings of 2013 IEEE Grenoble Conference*, Grenoble, France, Jun. 2013, pp. 1-5.

[12] L. He, C. Liu, A. Pitto *et al*., "Distance protection of AC grid with HVDC-connected offshore wind generators," *IEEE Transactions on Power Delivery*, vol. 29, no. 2, pp. 493-500, Apr. 2014.

[13] C. Chompoo-Inwai, C. Yingvivatanapong, K. Methaprayoon *et al*., "Reactive compensation techniques to improve the ride-through capability of wind turbine during disturbance," *IEEE Transactions on Industry Applications*, vol. 41, no. 3, pp. 666-672, May 2005.

[14] A. A. Abou El-Ela, A. M. Kinawy, M. T. Mouwafi *et al*., "Optimal siting and sizing of capacitors for voltage enhancement of distribution systems," in *Proceedings of 2015 50th International Universities Power Engineering Conference (UPEC)*, Stoke on Trent, Britain, Sept. 2015, pp. 1-6.

[15] S. Sundhararajan and A. Pahwa, "Optimal selecti of capacitors for radial distribution systems using a genetic algorithm," *IEEE Transactions on Power Systems*, vol. 9, no. 3, pp. 1499-1507, Aug. 1994.

[16] A. A. El-Fergany and A. Y. Abdelaziz, "Efficient heuristic-based approach for multi-objective capacitor allocation in radial distribution networks," *IET Generation, Transmission and Distribution*, vol. 8, no. 1, pp. 70-80, Jan. 2014.

[17] L. D. Jaffe, "Availability of solar and wind generating units," *IEEE Transactions on Power Apparatus System*, vol. PAS-104, no. 5, pp. 1012-1016, May 1985.

[18] J. Cao, W. Du, H. Wang *et al*., "Minimization of transmission loss in meshed AC/DC grids with VSC-MTDC networks," *IEEE Transactions on Power Systems*, vol. 28, no. 3, pp. 3047-3055, Aug. 2013.

[19] J. Beerten, S. Cole, and R. Belmans, "A sequential AC/DC power flow algorithm for networks containing multi-terminal VSC HVDC systems," in *Proceedings of IEEE PES General Meeting*, Minneapolis, USA, Jul. 2010, pp. 25-29.

[20] A. Rabiee, A. Soroudi, and A. Keane, "Information gap decision theory based OPF with HVDC connected wind farm," *IEEE Transactions on Power Syst*ems, vol. 30, no. 6, pp. 3396-3406, Nov. 2015.

[21] K. Y. Lee, Y. M. Park, and J. L. Ortiz, "A united approach to optimal real and reactive power dispatch," *IEEE Transactions on Power Apparatus Systems*, vol. PAS-l04, no. 5, pp.1147-1153, May 1985.

[22] Alireza Soroudi. (2020, Oct.). Power system optimization modeling in

GAMS. [Online]. Available: https://www. springer. com/gp/book/9783319623498
[23] G. Daelemans, K. Srivastava, M. Reza *et al*., "Minimization of steady-state losses in meshed networks using VSC HVDC," in *Proceedings of 2009 IEEE PES General Meeting*, Calgary, USA, Jul. 2009, pp. 1-5.
[24] A. Pizano-Martinez, C. R. Fuerte-Esquivel, H. Ambriz-Perez *et al*., "Modeling of VSC-based HVDC systems for a Newton-Raphson OPF algorithm," *IEEE Transactions on Power Systems*, vol. 22, no. 4, pp. 1794-1803, Nov. 2007.
[25] Richard D. Christie. (1993, Jan.). Power systems test case archive. [Online]. Available: http://labs. ece. uw. edu/pstca/pf118/pg_tca118bus. htm
[26] J. Zhang, H. Cheng, L. Yao *et al*., "Study on siting and sizing of distributed wind generation," *Proceedings of the CSEE*, vol. 29, no. 16, pp. 1-7, Jun. 2009.
[27] The Crown Estate and the Offshore Renewable Energy Catapult. (2019, May). Guide to an offshore wind farm. [Online]. Available: https://www. thecrownestate. co. uk/media/2861/guide-to-offshore-wind-farm-2019.pdf
[28] ETAP Operation Techonology Incoperated. (2017, Jun.). Optimal capacitor placement costs benefits due to loss reductions. [Online]. Available: https://etap. com/docs/default-source/white-papers/optimal-capacitor-placement-benefits.pdf?sfvrsn=4

Yong Li received the B. Sc. degree in electrical engineering from Hunan University, Changsha, China, in 2004, and the Ph.D. degree from TU Dortmund University, Dortmund, Germany, in 2012. He is currently a Professor with the College of Electrical and Information Engineering, Hunan University. His research interests include active distribution network operation, and analysis and control of power system stability and power quality.

Xuebo Qiao received the B.Sc. and M.S. degrees in electrical engineering from Hunan University, Changsha, China, in 2015 and 2018, respectively, where he is currently pursuing the Ph.D. degree. His research interests include planning and operation of transmission/distribution networks and integrated energy system.

Chun Chen received the B. Eng. degree in electrical engineering from Changsha University of Science & Technology, Changsha, China, in 2010, and the Ph. D. degree from Hunan University, Changsha, China, in 2016. His research interests include smart distribution network optimization and self-healing control.

Yi Tan received the B. Sc. degree in electrical engineering from the South China University of Technology, Guangzhou, China, in 2009, and the Ph.D. degree in electrical engineering from Hunan University, Changsha, China, in 2014. He is currently an Associate Professor with the College of Electrical and Information Engineering, Hunan University. His research interests include distribution network scheduling and the application of heuristic optimization and stochastic optimization in power systems.

Wenchao Tian received the B. Sc. degree in electrical engineering from Changsha University of Science & Technology, Changsha, China, in 2015, and the M.S. degree in electrical engineering from Hunan University, Changsha, China, in 2018. He is currently with the Zhangjiakou Power Supply Company, State Grid Jibei Electric Power Company Limited, Zhangjiakou, China. His research interests include planning and operation of power systems.

Qiuping Xia received the B. Sc. degree in electrical engineering from Guizhou University, Guiyang, China, in 2015, and the M.S. degree in electrical engineering from Hunan University, Changsha, China, in 2018. She is currently with the Zhangjiakou Power Supply Company, State Grid Jibei Electric Power Company Limited, Zhangjiakou, China. Her research interests include stability and power quality analysis in power systems.

Yijia Cao received the B.Sc. degree in electrical engineering from Xi'an Jiaotong University, Xi'an, China, in 1988, and the Ph.D. degree from Huazhong University of Science and Technology, Wuhan, China, in 1994. He is currently a Professor with the College of Electrical and Information Engineering, Hunan University, Changsha, China. His research interests include power system cascading failure, smart grid information technology, and smart grid optimization.

Kwang Y. Lee received the B. S. degree from Seoul National University, Seoul, Korea, in 1964, and the M.S. degree from North Dakota State University, Fargo, in 1968, both in electrical engineering, and the Ph.D. degree in system science from Michigan State University, East Lansing, USA, in 1971. He is currently a Professor and Chair of electrical and computer engineering with Michigan State University; Oregon State University, Corvallis, USA; University of Houston, Houston, USA; The Pennsylvania State University, University Park, USA; and Baylor University, Waco, USA. His current research interests include power system control, operation, planning, and intelligent system applications to power systems.